



Rational design of Tamiflu derivatives targeting at the open conformation of neuraminidase subtype 1

Yan Li, Bingcheng Zhou, Renxiao Wang*

State Key Laboratory of Bioorganic Chemistry, Shanghai Institute of Organic Chemistry, Chinese Academy of Sciences, 345 Lingling Road, Shanghai 200032, PR China

ARTICLE INFO

Article history:

Received 10 April 2009

Received in revised form 30 June 2009

Accepted 4 July 2009

Available online 4 August 2009

Keywords:

Neuraminidase subtype 1

Fragment-based design

Tamiflu

Molecular docking

Molecular dynamics simulation

ABSTRACT

Neuraminidase is an attractive therapeutic target for standing against influenza virus, such as the threatening avian influenza virus H5N1. A recently discovered cavity near the well-known catalytic site on neuraminidase subtype 1 (N1) provides a good possibility to develop dual-site-binding inhibitors, which may achieve improved activities and selectivities against N1. We have designed some derivatives of Tamiflu with such features through a fragment-based approach combining multiple computational methods. Over 1000 FDA-approved small-molecule drugs were computationally screened targeting at the open conformation of N1 with the GOLD program in combination with the X-Score scoring function. Some chemical fragments on the top-scored hits, which were able to fit into the 150-cavity, were transplanted onto the core structure of Tamiflu to produce a total of 30 new molecules. Then, binding of these designed molecules to N1 was evaluated by molecule docking. The promising ones were further subjected to molecular dynamics simulation of 3 ns long, and their binding free energies were computed by using the MM-PB/SA method. Some of our designed molecules were predicted to have comparable or even better binding affinities than that of Tamiflu. We report our results herein so that other researchers who have the necessary chemical and biological resources can utilize them in the development of new N1 inhibitors. In addition, our study actually suggests a practical strategy for optimizing a given lead compound based on the outcomes of a standard virtual screening trial.

© 2009 Elsevier Inc. All rights reserved.

1. Introduction

Some worst epidemics in human history were caused by influenza viruses. Influenza viruses contain two major surface glycoproteins: haemagglutinin and neuraminidase. Haemagglutinin is responsible for attaching the virus to host cells via sialic acid binding sites and promoting viral fusion [1]. After virus replication, neuraminidase cuts off the link between haemagglutinin and the receptors containing sialic acid on the host cells to facilitate the release and spread of new virus particles [2]. According to different antigenic properties of haemagglutinin and neuraminidase molecules, influenza type A viruses can be classified into 16 subtypes by haemagglutinin (H1–H16) and 9 subtypes by neuraminidase (N1–N9) [3]. Numerous combinations of haemagglutinin and neuraminidase subtypes have been found in influenza type A viruses on avian species, i.e. bird flu. Among them, H5N1 has received extensive attention in recent years since it has caused a considerable number of human lives worldwide [4]. In theory, both haemagglutinin and neuraminidase can be considered as

therapeutic targets for preventing the replication and spread of influenza viruses in host cells. Although the crystal structure of haemagglutinin was already resolved in early 1980s [5], no tightly binding compounds have been discovered for it. As for neuraminidase, many inhibitors with high potencies have been developed. For example, zanamivir and oseltamivir (Tamiflu) are two successful drugs currently in use [6,7]. Nevertheless, resistance against these drugs has subsequently been developed by influenza viruses, still making the development of new classes of neuraminidase inhibitors a significant and urgent task [8].

Most known neuraminidase inhibitors are developed by referring to the binding mode observed in the N9–DANA complex (Fig. 1). The binding site of neuraminidase has four characteristic features, which are largely conserved [9]: (1) A basic subsite formed by Arg118, Arg292 and Arg371. In the case of the DANA–N9 complex, this subsite forms salt bridges with a carboxylic group on DANA. (2) An acidic subsite formed by Glu119 and Asp151, interacting with a polar group (such as amide or hydroxyl) at the C4-position on the ligand. (3) A hydrogen bond formed by Arg152 with a conserved acetyl amide group at the C5-position on the ligand. (4) A subsite accommodating the glycerol moiety on DANA. In the case of Tamiflu binding, it can change into a hydrophobic subsite after a conformational rearrangement of Glu276 to form a

* Corresponding author. Tel.: +86 21 54925128.

E-mail address: wangrx@mail.sioc.ac.cn (R. Wang).

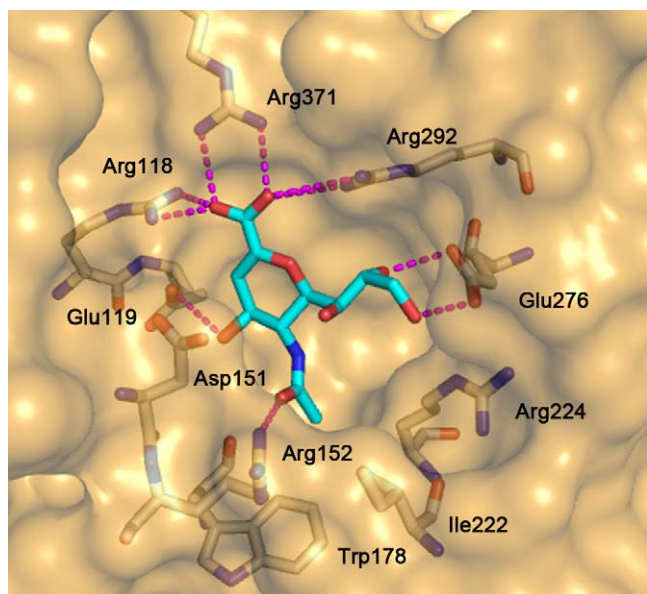
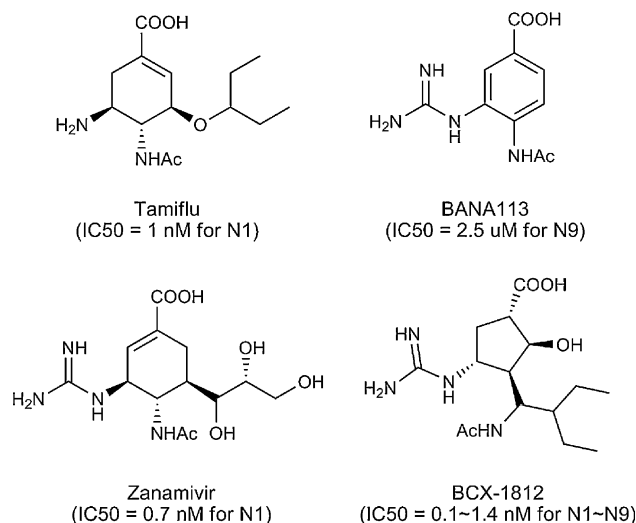


Fig. 1. Binding mode of 2-deoxy-2,3-didehydro-N-acetylneuraminic acid (DANA) with N9 (PDB entry: 1F8B). Major amino acid residues involving in N9–DANA are rendered in stick models. The dashed lines indicate the hydrogen bonds formed between N9 and DANA.

salt bridge with Arg224 [7]. The major strategy of structural optimization of neuraminidase inhibitors during the last decade has focused on the chemical moieties occupying the glycerol binding subsite to improve binding affinities and bioavailabilities of the designed molecules [10,11]. Modifications on other positions are also possible [12]. Scheme 1 shows the chemical structures of some representative neuraminidase inhibitors. In these compounds, the carboxylic and amide groups are kept down with varieties of scaffolds from cyclohexenyl and phenyl to cyclopentane and pyrrole [13–17].

In 2006, the Russell group released the X-ray crystal structures of N1 both in *apo*- and *holo*-forms for the first time [18]. Their structures indicate that N1 has quite different conformations around the known active site (Fig. 2). Compared to N2 and N9, N1 may have an additional cavity near the 150-loop region, the “150-cavity”, approximately 10 Å long and 5 Å wide. Incubating N1 crystals in 20 μM Tamiflu results in a relatively extended conformation of the 150-loop, making the 150-cavity exposed to the solvent. We will refer to this particular conformation of N1 as the “open conformation” throughout this paper. If the crystal is grown with a higher concentration of Tamiflu, the 150-loop takes a more compact conformation and the 150-cavity basically disappears. We will refer to this particular conformation of N1 as the “closed conformation” throughout this paper. As implied above, both the open and closed conformations of N1 are stable under certain conditions. Therefore, the open conformation of N1 can be utilized as the structural target for designing new classes of N1 inhibitors. If an N1 inhibitor occupies both the main binding site and the newly discovered 150-cavity, it is possible to achieve higher binding affinity than known N1 inhibitors since it may form more interactions with N1. In addition, since this 150-cavity has not been observed on other subtypes of neuraminidase, such compounds may also have a good selectivity towards N1. Though some compounds that work against all neuraminidase subtypes are also desired, effective and specific N1 inhibitors may be more practical to stand against the present avian influenza virus H5N1. This is the origin of our idea presented in this paper.

Some other researchers have also proposed similar strategies for designing new classes of N1 inhibitors by targeting at the open conformation of N1. To the best of our knowledge, two such studies



Scheme 1. Some known neuraminidase inhibitors for treating influenza A virus.

have been published while our manuscript was in preparation. Garcia-Sosa et al. [19] conducted a virtual screening of a total of 67 768 compounds from three databases (DrugBank, NCI diversity set, and ZINC) to select the ones that targeted simultaneously at the adjacent binding sites on the open conformation of N1. By considering predicted binding free energies, ligand efficiency values, and consensus scoring, they suggested a variety of chemical structures as potential N1 inhibitors. Amaro et al. [20] conducted extensive molecular dynamics simulations of *apo*- and *holo*-forms of N1 to derive six most dominant conformations of N1. These MD snapshots, together with two crystal structures, were then used in subsequent virtual screening of the NCI diversity set (~2000 compounds) to identify multi-site binding compounds. The authors claimed that “the use of the MD-generated structures systematically incorporates a broader range of receptor configurations into the hit identification process”. Finally, a total of 27 top hits were selected, which were able to bind with the ensemble of all 8 N1 conformations.

Although our design was also based on the open conformation of N1, we adopted a quite different approach to derive the desired new N1 inhibitors from the very beginning. Both studies mentioned above relied on virtual screening to find some novel chemical structures that may be multi-site binders of N1. The computational techniques employed in both studies were reasonable. However, considering the unpredictable success rates of virtual screening, one may or may not find some promising compounds among the top hits selected by the authors. The value of these two studies cannot be fully justified until the biological activities of these hits are actually tested in experiments. In contrast, we took the core structure of Tamiflu, assuming that it would still occupy the main binding site, and then added some appropriate chemical fragments onto this structure to extend into the adjacent 150-cavity. In other words, we developed the structure of Tamiflu to obtain new dual-site-binding N1 inhibitors. Since Tamiflu is a well-known effective binder to both the closed and open conformations of N1, we expect that our designed molecules are more likely to exhibit the desired biological activities towards N1. In addition, since Tamiflu is an approved drug for treating influenza virus, Tamiflu-based compounds may have advantages with respect to pharmacokinetics properties and toxicity.

In our study, we first determined through a set of validations that GOLD/GoldScore was the suitable molecular docking tool for modeling the binding modes of N1 inhibitors. With this docking/scoring scheme, we then conducted a virtual screening of over 1000 small-molecule drugs approved by FDA against the open conformation of N1. The top hits were visually examined, and some

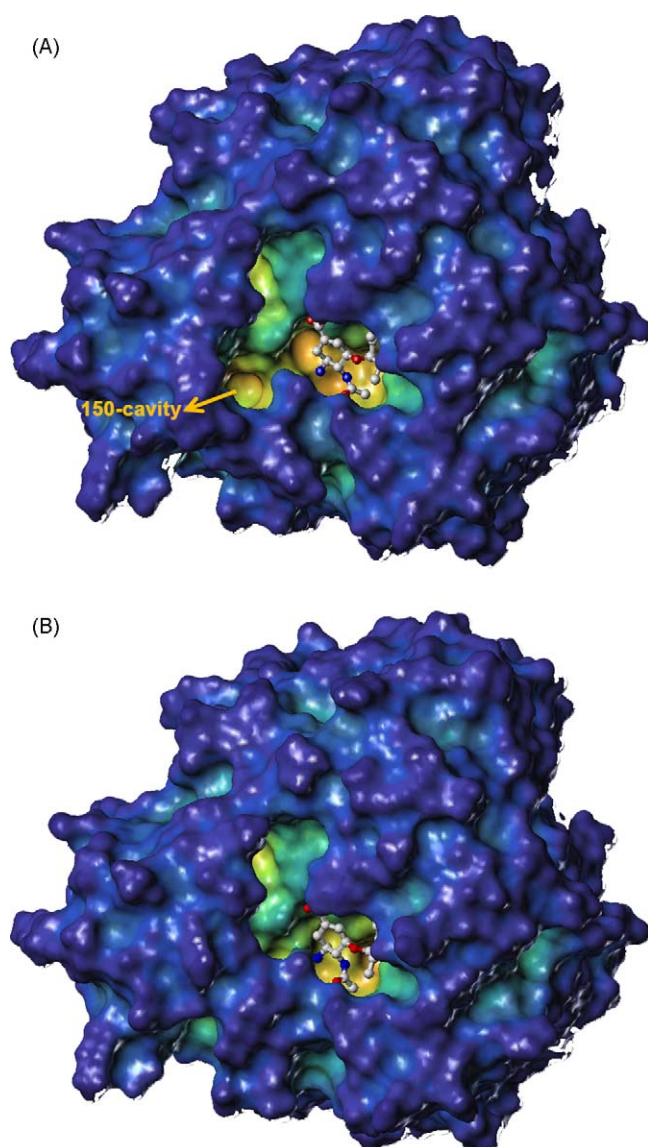


Fig. 2. Crystal structures of N1–Tamiflu complexes in the open conformation (PDB entry 2HU4, A) and the closed conformation (PDB entry 2HU4, B). Tamiflu is rendered in the ball-and-stick model. Cavities on the protein surface are indicated in light colors.

appropriate chemical fragments were truncated from them and transplanted onto the core structure of Tamiflu. A total of 30 new molecules were sketched after necessary manual modifications. The binding modes of these new molecules were further refined by molecular dynamics simulations in explicit solvent. Binding free energies of these molecules were assessed by scoring functions as well as the MM-PB/SA method. Some interesting molecules among the final outcomes were identified. In particular, a class of compounds containing a substituted furan moiety seem to be promising. The possible synthetic route of this class of compounds is also proposed. We reveal our results to the public so that other researchers who possess the necessary chemical and biological resources may test them experimentally.

2. Methods

2.1. Validation of docking/scoring methods

It is well known that the performance of different docking/scoring methods may vary among different systems [21–24]. The

first step of our work therefore was to test the docking/scoring methods available to us to find out the optimal scheme for evaluating the binding of N1 inhibitors. For this purpose, a total of 46 Tamiflu-like N1 inhibitors were selected from literatures (Table 1) [13,25]. All their biological data (IC_{50}) were determined in identical bioassays conducted by the same group. These molecules were sketched by using the Sybyl software (version 7.2, Tripos Inc.), and their three-dimensional structures were optimized with the MMFF94 force field. Two crystal structures of the N1–Tamiflu complexes were retrieved from the Protein Data Bank [26], representing the open conformation of N1 (PDB entry 2HU0) and the closed conformation of N1 (PDB entry 2HU4), respectively. Since these 46 N1 inhibitors are basically analogues of Tamiflu, we assumed that they bound to the closed conformation of N1, the thermodynamically more stable form of N1, just like Tamiflu. Therefore, our subsequent validations of docking/scoring methods were all based on the closed conformation of N1 as in PDB entry 2HU4.

All 46 molecules, including Tamiflu, were docked into the binding site on N1 by using two molecular docking programs, including the GOLD program (version 3.1, released by the Cambridge Crystallographic Data Center) and the LigandFit module implemented in the Discovery Studio software suite (version 1.7, released by the Accelrys Inc.). GOLD [27] relies on a genetic algorithm to perform conformational sampling. Two scoring functions, namely GoldScore [28] and ChemScore [29], are implemented in GOLD for ranking ligand binding poses. LigandFit [30] is basically a shape-based docking method. It adopts a Monte Carlo algorithm to perform conformational sampling and a force field-based method for evaluating ligand binding poses. In our study, the main docking parameters were set as follows: For GOLD, the binding site was composed of the residues within 15 Å from Tamiflu in the given crystal structure. A docking protocol with 300 000 GA cycles was run with GoldScore and ChemScore, respectively. Thirty binding poses were retained for each given ligand; for LigandFit, definition of the binding site was also based on the coordinates of Tamiflu in the given crystal structure. The CFF force field was used for energy calculations. The number of Monte Carlo sampling cycles was set to 20 000. A maximal of 30 binding poses were also retained for each given ligand. If not specified above, other parameters were set as default in our application of GOLD and LigandFit.

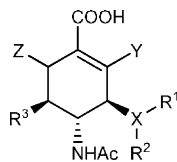
After molecular docking, the output binding poses were visually inspected. The binding poses with optimal binding scores and reasonable interactions with N1 were manually selected and rescored using all the scoring functions mentioned above. After the binding poses of all 46 N1 inhibitors were determined, a total of eight scoring functions were applied to them to compute their binding scores. These scoring functions included GoldScore and ChemScore implemented in GOLD (version 3.1), PLP [31], PMF [32], LigScore [33], Ludi [34], and Jain [35] implemented in the Discovery Studio software (version 1.7), and X-Score (version 1.3) [36]. Correlation coefficients between the binding scores given by each scoring function and the experimental binding data ($-\log_{10} IC_{50}$) were calculated. The results are summarized in Table 2. The docking method that best reproduced the binding modes of N1 inhibitors and the scoring function that offered the best correlation coefficient were considered as the appropriate combination for evaluating N1 inhibitors in subsequent analyses: they were GOLD/GoldScore for molecular docking and X-Score for rescored.

2.2. CoMFA model of Tamiflu-like N1 inhibitors

Comparative Molecular Field Analysis (CoMFA) [37] is another approach for studying the quantitative structure–activity relation-

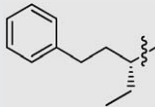
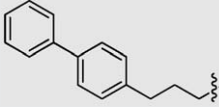
Table 1

Chemical structures and biological activities of 46 Tamiflu-like N1 inhibitors.



ID	X	Y	Z	R ¹	R ²	R ³	IC ₅₀ (nM)
1	O	-H	-H	-H	-	-NH ₂	6300
2	O	-H	-H	-CH ₃	-	-NH ₂	3700
3	O	-H	-H	-CH ₂ CH ₃	-	-NH ₂	2000
4	O	-H	-H	-(CH ₂) ₂ CH ₃	-	-NH ₂	180
5	O	-H	-H	-(CH ₂) ₃ CH ₃	-	-NH ₂	300
6	O	-H	-H	-CH ₂ OCH ₃	-	-NH ₂	2000
7	O	-H	-H	-CH ₂ CH=CH ₂	-	-NH ₂	2200
8	O	-H	-H	-(CH ₂) ₂ CF ₃	-	-NH ₂	225
9	O	-H	-H	-(R)-CH(CH ₃)CH ₂ CH ₃	-	-NH ₂	10
10	O	-H	-H	-(S)-CH(CH ₃)CH ₂ CH ₃	-	-NH ₂	9
11	O	-H	-H	-CH ₂ CH(CH ₃) ₂	-	-NH ₂	200
12	O	-H	-H		-	-NH ₂	1
13	O	-H	-H		-	-NH ₂	3
14	O	-H	-H		-	-NH ₂	1
15	O	-H	-H		-	-NH ₂	22
16	O	-H	-H		-	-NH ₂	60
17	O	-H	-H		-	-NH ₂	16
18	O	-H	-H		-	-NH ₂	1
19	O	-H	-H		-	-NH ₂	530
20	O	-H	-H		-	-NH ₂	620
21	O	-H	-H		-	-NH ₂	0.3

Table 1 (Continued)

ID	X	Y	Z	R ¹	R ²	R ³	IC ₅₀ (nM)
22	O	–H	–H		–	–NH ₂	12
23	O	–H	–H		–	–NH ₂	90
24	O	–H	–H	–H	–	–NHC(=NH)NH ₂	100
25	O	–H	–H	–(CH ₂) ₂ CH ₃	–	–NHC(=NH)NH ₂	2
26	O	–H	–H	–(CH ₂) ₃ CH ₃	–	–NHC(=NH)NH ₂	3
27	O	–H	–H	–(R)–CH(CH ₃)CH ₂ CH ₃	–	–NHC(=NH)NH ₂	0.5
28	O	–H	–H	–(S)–CH(CH ₃)CH ₂ CH ₃	–	–NHC(=NH)NH ₂	0.5
29	O	–H	–H	–CH(CH ₂ CH ₃) ₂	–	–NHC(=NH)NH ₂	0.5
30	O	–H	–H	–CH(CH ₂ CH ₃) ₂	–	–NH ₂	1
31	O	–CH ₃	–H	–CH(CH ₂ CH ₃) ₂	–	–NH ₂	2300
32	O	–F	–H	–CH(CH ₂ CH ₃) ₂	–	–NH ₂	3
33	O	–H	–CH ₃	–CH(CH ₂ CH ₃) ₂	–	–NH ₂	1500
34	N	–H	–H	–(CH ₂) ₂ CH ₃	–CH ₃	–NH ₂	65
35	N	–H	–H	–(CH ₂) ₃ CH ₃	–CH ₃	–NH ₂	180
36	N	–H	–H	–CH(CH ₂ CH ₃) ₂	–CH ₃	–NH ₂	6
37	N	–H	–H	–(CH ₂) ₂ Ph	–CH ₃	–NH ₂	100
38	N	–H	–H	–c-C ₆ H ₁₁	–CH ₃	–NH ₂	200
39	N	–H	–H	–(CH ₂) ₂ CH ₃	–CH ₂ CH ₃	–NH ₂	90
40	N	–H	–H	–(CH ₂) ₃ CH ₃	–CH ₂ CH ₃	–NH ₂	85
41	N	–H	–H	–(CH ₂) ₂ CH ₃	–(CH ₂) ₂ CH ₃	–NH ₂	12
42	N	–H	–H	–(CH ₂) ₂ CH ₃	–H	–NH ₂	200
43	N	–H	–H	–CH(CH ₂ CH ₃) ₂	–H	–NH ₂	11
44	N	–H	–H	–COCH ₂ CH ₃	–H	–NH ₂	2700
45	N	–H	–H	–COCH(CH ₃) ₂	–H	–NH ₂	6400
46	N	–H	–H	–COCH(CH ₂ CH ₃) ₂	–H	–NH ₂	4000

^aThe IC₅₀ data of compounds 1–33 and 34–46 are cited from Refs. [13,25], respectively.

ships of bioactive compounds. In our study, the results from a CoMFA model were compared with those of docking/scoring methods. Tamiflu as well as 45 Tamiflu-like N1 inhibitors were subjected to CoMFA analysis, in which the binding poses of these molecules produced at the previous step were used to derive the CoMFA model. CoMFA steric and electrostatic interaction fields were calculated using the default parameters defined in the Sybyl software. The cutoff values for the steric and electrostatic fields were both set to 30.0 kcal/mol. The CoMFA model was derived through a partial-least-squares regression, in which the steric and electrostatic fields were used as the independent variables and $-\log_{10} IC_{50}$ values of these molecules were used as the dependent variable. A leave-one-out cross-validation was also conducted to assess the predictive power of this CoMFA model.

Table 2

Correlations between the experimental binding data of 46 N1 inhibitors and the binding scores computed by different scoring functions.

Scoring function	R	SD ^a
X-Score	0.740	0.88
PLP2	0.723	0.91
PLP1	0.711	0.92
LUDI2	0.697	0.95
GoldScore	0.690	0.95
LUDI3	0.662	0.98
PMF	0.651	0.99
LUDI1	0.648	1.00
ChemScore	0.505	1.13
Jain	0.479	1.15
LigScore1	0.402	1.20
LigScore2	0.344	1.23

^a In log IC₅₀ units.

2.3. Fragment-based molecular design

Fragment-based design [38–41] has become a popular strategy in structure-based drug design. Our basic idea for designing a new class of N1 inhibitors was to attach some appropriate fragments to the core structure of Tamiflu, assuming that the latter would still occupy the main binding site while the attached fragments would occupy the 150-cavity on the open conformational of N1. Since the 150-cavity was relatively small, virtual screening of a chemical fragment library may not find suitable and diverse hits particularly fitting to this site. Instead, we chose to screen a library of drug molecules through molecular docking towards the entire binding site (the main binding site plus the 150-cavity), truncate the appropriate fragments occupying the 150-cavity from these molecules, and then transplant them onto the core structure of Tamiflu or other active compounds. After necessary structural modifications, it is possible to obtain dual-site-binding ligand molecules for N1. This process is illustrated conceptually in Fig. 3.

In our study, a total of 1046 small-molecule drugs approved by the Food and Drug Administration (FDA) of the United States were considered in virtual screening. The information of these drug molecules were downloaded from the DrugBank database [42]. As prompted by the results of the previous validation step, the GOLD/GoldScore method was employed to dock all these molecules towards the binding site on the open conformational of N1. The docking parameters were set as follows: The binding site was defined to be composed of residues within 5.0 Å from a hypothetical reference molecule, which was manually constructed based on Tamiflu to fill up the main binding site as well as the 150-cavity. A total of 100 000 GA operations were run for each given molecule, and the top three binding poses were retained for

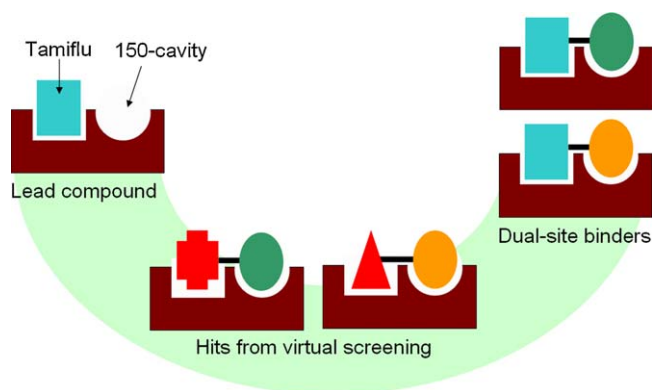


Fig. 3. Schematic illustration of our fragment-based design approach: suitable chemical fragments fitting the 150-cavity are truncated from the candidates molecules selected by a standard virtual screening trial against N1. They are then transplanted onto the core structure of Tamiflu to obtain new dual-site binders to N1.

subsequent selection. Only the binding poses with binding scores higher than 40.0 were considered since we observed that very few binding poses with binding scores lower than this cutoff could fill up the 150-cavity. For all of the qualified candidates, we then manually truncated the fragments occupying the 150-cavity from them by breaking the chemical bond at appropriate positions, and then transplanted them onto the core structure of Tamiflu by making new chemical bonds as necessary. Some atom/bond types were changed accordingly at this step to keep the validity of the new structures. Binding modes of these newly designed molecules were then optimized *in situ* within the binding site of N1 by using the MMFF94 force field in the Sybyl software. Binding affinities of these molecules were computed by GoldScore in GOLD as well as the X-Score program based on the predicted binding mode of each molecule.

2.4. Molecular dynamics simulations

MD simulations were used to further refine the binding modes of our designed molecules to N1 since the N1 structure of was kept fixed during our molecular docking studies at the previous step. The binding pose of each designed N1 inhibitor (the ligand) selected at the previous step was used as the starting conformation for MD simulation. The electrostatic potentials of each ligand were obtained through single-point energy calculation at the HF/6-31g (d) level by using the Gaussian03 program [43], and then the atomic partial charges on the ligand were derived by the RESP method [44] in the AMBER program (version 9) [45]. Atomic partial charges on the amino acid residues on N1 used the AMBER FF03 template charges. The protonation states of all amino acid residues with ionizable side chains, including Asp, Glu, Arg, Lys, and His, were set as the default states at pH = 7.

After these preparations, each N1 complex was soaked in a cubic box filled with TIP3P water molecules, in which any atom on the N1 complex was at least 10 Å away from any face of the box. An appropriate number of sodium ions were added to neutralize the entire system. All MD simulations were performed by using the SANDER module in the AMBER program. FF03 and GAFF force field parameters were applied to N1 and the ligands, respectively. First, the complex structure was relaxed by 100 cycles of steepest descent minimization, followed by 4900 cycles of conjugated gradient minimization. The convergence criterion was set to 0.01 kcal/(mol Å). After that, the systems were gradually heated up with the Berendsen algorithm [46] from 0 K to 300 K in 120 ps. Then, 3 ns MD simulation was performed for each complex at a constant temperature of 300 K and a constant pressure at 1 atm. Electrostatic

interactions were calculated with the PME algorithm [47]. The distance cutoff of non-bonded interactions was set to 12 Å. The SHAKE algorithm [48] was applied to fix the lengths of all chemical bonds connecting hydrogen atoms. No other restraints were applied during the simulation. The resulting MD trajectory of each complex was used in binding free energy computation at the next step.

2.5. Computation of binding free energies

The MM-PB/SA method is used to calculate the binding free energies between N1 and all designed molecules. MM-PB/SA method is a popular method for the computation of protein–ligand binding free energies, which was firstly developed by Kollman et al. in 2000s [49]. A good number of successful applications of the MM-GB(PB)/SA methods have already reported in the literature [50–56]. The principle of MM-PB/SA is based on the thermodynamic cycle of protein–ligand binding. It can be conceptually summarized as:

$$\Delta G_{\text{bind}} = \langle G_{\text{complex}} - G_{\text{protein}} - G_{\text{ligand}} \rangle \quad (1)$$

$$G \approx E_{\text{gas}} - TS_{\text{conf}} + G_{\text{sol}} \quad (2)$$

$$E_{\text{gas}} = E_{\text{bond}} + E_{\text{angle}} + E_{\text{torsion}} + E_{\text{vdw}} + E_{\text{elec}} \quad (3)$$

$$G_{\text{sol}} = G_{\text{elec}} + G_{\text{non-polar}} \quad (4)$$

Here, the binding free energy change in protein–ligand binding (ΔG_{bind}) is computed as the difference between the free energies of the complex (G_{complex}), the protein (G_{protein}), and the ligand (G_{ligand}). The free energy of each molecule is calculated through Eq. (2) by summing up its internal energy in the gas phase (E_{gas}), the solvation free energy (G_{sol}), and a vibrational entropy term (S_{conf}) computed by the normal mode analysis. E_{gas} is a standard force field energy, including strain energies from covalent bonds and torsion angles as well as non-covalent van der Waals and electrostatic energies (Eq. (3)). The solvation free energy (G_{sol}) is computed as the sum of an electrostatic component, and a non-polar component (Eq. (4)). The electrostatic component is computed by the Poisson–Boltzmann (PB) method [57,58] while the non-polar component is assumed to be proportional to the solvent-accessible surface area (SASA) of the molecule under consideration. As indicated by the angled brackets in Eq. (1), a distinctive feature of MM-PB/SA is that it computes the averages of all of the above properties over a configurational ensemble, which is typically generated through MD simulations of the given protein–ligand complex. In our study, the internal energy (E_{gas}) of each given molecule was computed by the General AMBER Force Field (GAFF). The electrostatic term in the solvation free energy (G_{elec}) was calculated by the PBSA module in the AMBER program. The same set of atomic charges on each complex used in MD simulation was used in PB computations. The dielectric constant was set to 1 inside the solute and 80 in solvent. The non-polar term in solvation free energy was computed as $G_{\text{non-polar}} = \beta \times \text{SASA} + \gamma$. Here, SASA is the solvent-accessible surface area (SASA) of each given molecule, which was computed using the MOLSURF module in AMBER with a solvent probe radius of 1.4 Å. The parameter β was set to 0.0072 kcal/(mol Å²) and the parameter γ was set to zero according to the default setting by AMBER. The vibrational entropy S_{conf} was computed by using the NMODE module in AMBER.

For each complex, a total of 100 snapshots were retrieved from the last 1 ns segment on the MD trajectory with an even interval of 10 ps. The arithmetic averages of the internal energies and solvation free energies of each species in Eq. (1) were computed on this configurational ensemble. The vibra-

tional entropy term (S_{conf}) of each molecule was computed by using the NMODE module in AMBER9. Since computation of this term was quite time-consuming, it was computed on a total of 10 snapshots for instead, which were also retrieved from the last 1 ns segment of the MD trajectory with an interval of 100 ps. Combination of these three components, including the internal energies, produced the total binding free energy of each complex.

3. Results and discussions

3.1. Validation of docking/scoring methods

Molecular docking was employed as the essential tool in our study for modeling the binding modes of all known N1 inhibitors as well as the newly designed ones. Thus, it is critical for the success of our work to choose the appropriate docking and scoring methods applicable to the modeling of N1 inhibitors through validation. Our results indicated that molecular docking by the GOLD program (using GoldScore as the scoring function, i.e. GOLD/GoldScore) was able to successfully reproduce the observed binding modes of Tamiflu to N1 both on the open and closed conformations. The root-mean-square-deviation (RMSD) values between the best-scored binding poses and the observed binding poses of Tamiflu in crystal structures were 0.83 Å and 0.39 Å on the open and closed conformations, respectively (Fig. 4B and A). Molecular docking by GOLD/ChemScore or LigandFit was also able to reproduce the observed binding mode of Tamiflu on the closed conformation of N1, yielding RMSD values of 0.39 Å and 0.55 Å,

respectively (Fig. 4C and E). These two approaches, however, could not fully reproduce the observed binding mode of Tamiflu on the open conformation (Fig. 4D and F). We thus concluded that among all of the docking/scoring schemes under our test, GOLD/GoldScore was most suitable for modeling the binding of N1 inhibitors. In another set of validation, GOLD/GoldScore was applied to predict the binding poses of 46 known Tamiflu-like N1 inhibitors on the closed conformation of N1 (Table 1). The obtained binding poses of these compounds are all similar to that of Tamiflu. Hydrogen bonding interaction is obviously the dominant factor for maintaining the binding of these Tamiflu analogues to N1. The critical hydrogen bonds formed between these compounds and N1 include the ones between the carboxylic group on the core structure and three nearby Arg residues, including Arg118, Arg292, and Arg371. Thus, the reasonable performance of GOLD/GoldScore in determining the correct binding modes of N1 inhibitors in our study can be explained since GoldScore [28] is a scoring function with an emphasis on hydrogen bonding.

CoMFA was also applied to those 46 Tamiflu analogues in our study. Our CoMFA model was derived based on the binding

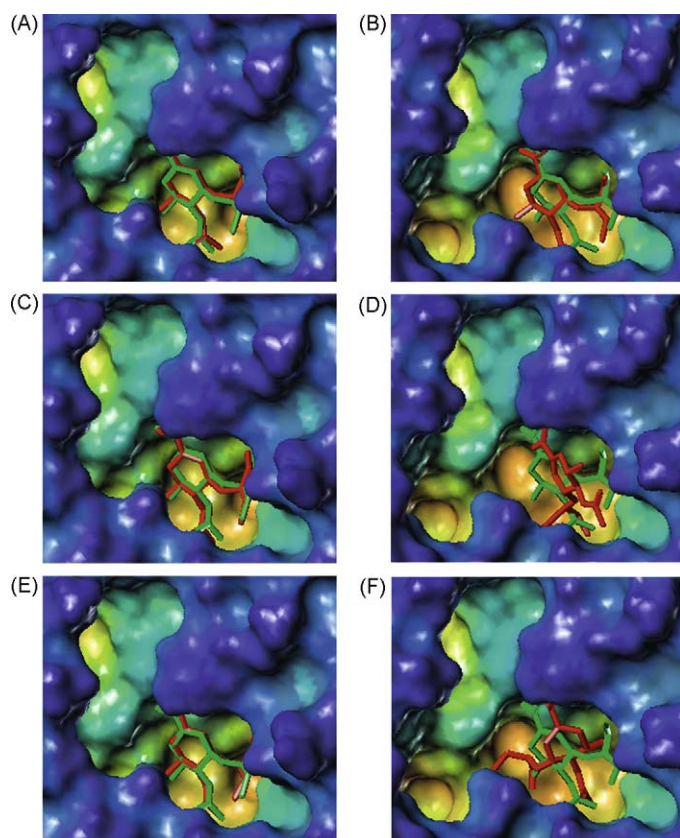


Fig. 4. Comparison of the observed binding poses of Tamiflu in crystal structures and the predicted binding poses by GOLD/GoldScore (A and B), GOLD/ChemScore (C and D), and LigandFit (E and F). Predicted binding poses are in red; while the observed ones are in green. Cavities on the protein surface are indicated in light colors. Results obtained on the closed conformation of N1 are illustrated in A, C, and E; while results obtained on the open conformation of N1 are illustrated in B, D, and F.

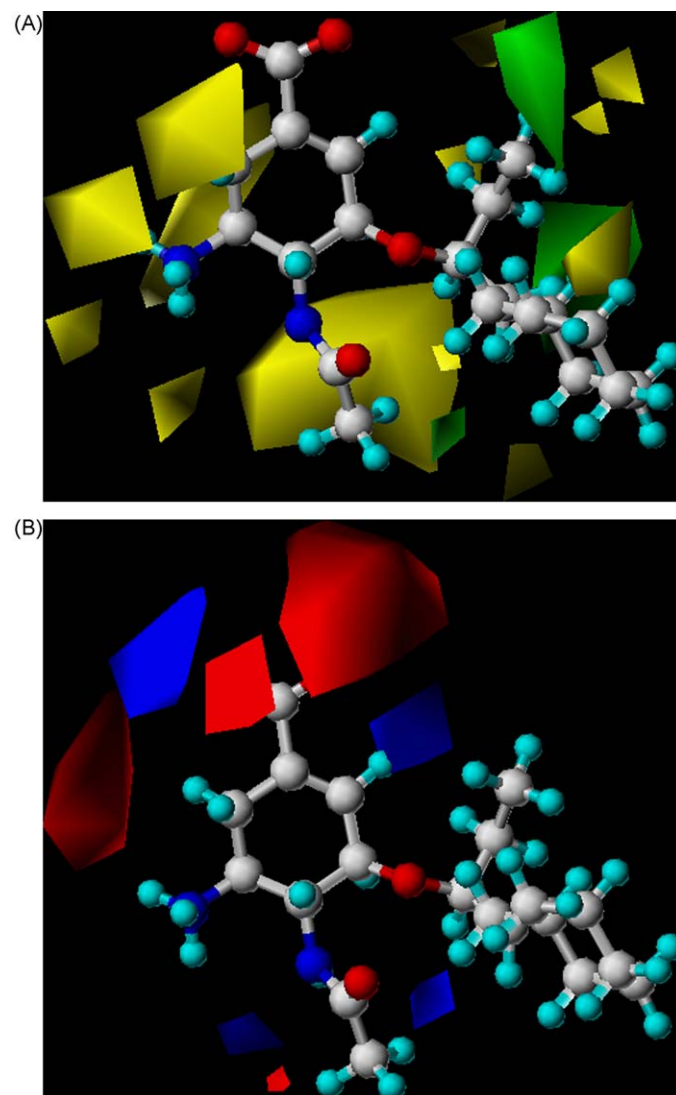


Fig. 5. Steric (A) and electrostatic (B) contours given by a CoMFA study of 46 Tamiflu analogues. Compound **18** is shown here as a representative. Steric contours are shown in green (favored region) and yellow (bulk disfavored region); while electrostatic contours are shown in red (negative charge favored region) and blue (positive charge favored region).

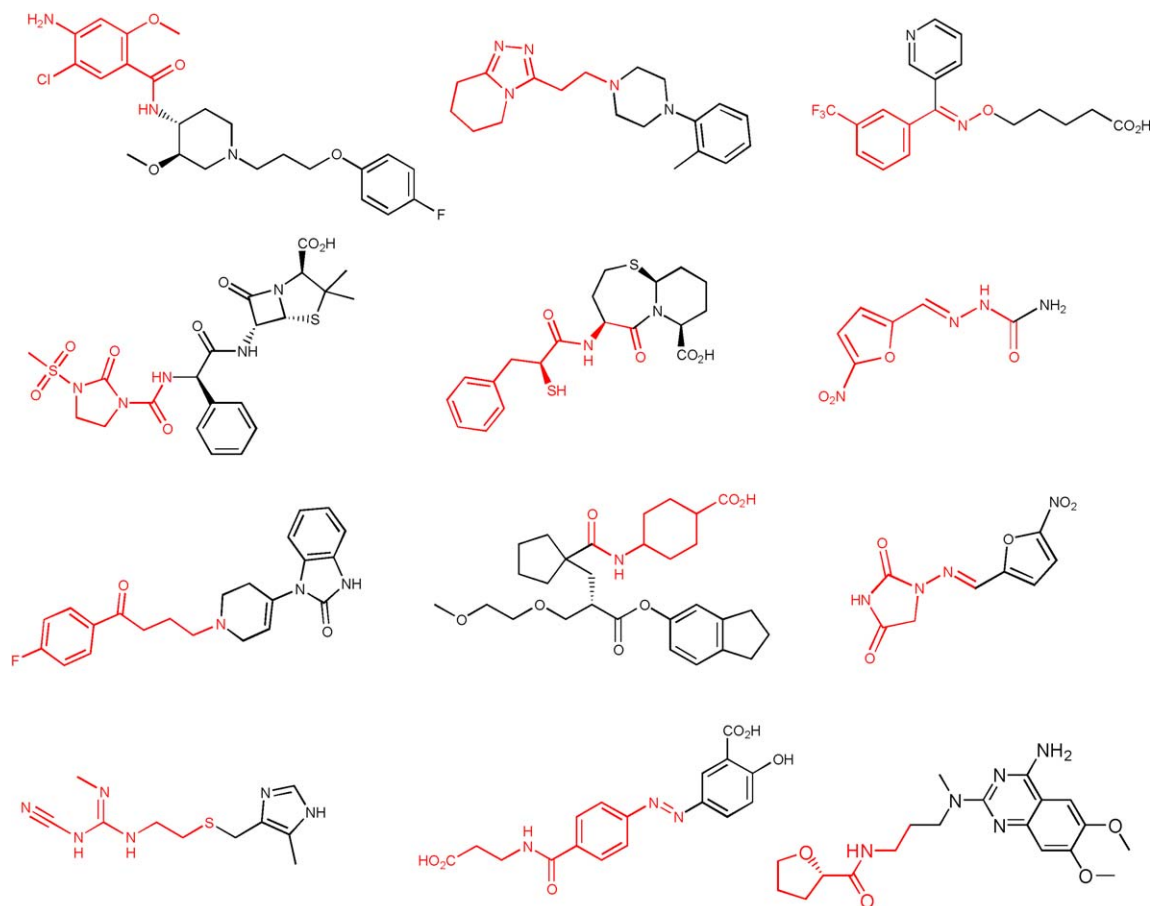
poses predicted by GOLD/GoldScore, serving as an additional evaluation of the performance of GOLD/GoldScore in this case. Our CoMFA model produced a significant correlation coefficient ($r^2 = 0.966$) with an optimal number of components of 6. This model also gave a good predictive correlation coefficient ($q^2 = 0.780$) between the biological activities and the CoMFA descriptors in the leave-one-out cross-validation trial. The steric and electrostatic fields given by this CoMFA model are illustrated in Fig. 5, in which one particular compound, compound **18** (Table 1), is used as an example to indicate their locations in space. On this figure, one can observe a favored region around the cyclohexyl substitution group on **18** for steric interactions, which is in agreement with the high activity of this compound ($IC_{50} = 1.0$ nM). Indeed, enhancing the steric interactions at this particular site is a practical strategy for improving the potencies of neuraminidase inhibitors [10,11]. One can also observe a major favored region for electrostatic interactions around the carboxyl group on the top of the core structure, corresponding to the interactions formed between this carboxyl group and the nearby Arg292 and Arg371 residues common to this set of compounds (see Fig. 1). Thus, the information derived from our CoMFA model is all in good agreement with the binding modes predicted by GOLD/GoldScore.

After the binding poses of these N1 inhibitors were set by GOLD/GoldScore, their binding affinities to N1 were evaluated by a total of eight scoring functions as described in Section 2. The Pearson correlation coefficients (R) between the experimental binding affinities ($-\log_{10} IC_{50}$) of these molecules and the corresponding binding scores given by all scoring functions are summarized in Table 2. One can see that the performance of these scoring

functions on this set of compounds was obviously on different levels. The best one among them was X-Score, which produced a reasonable correlation ($R = 0.740$) between experimental and computed binding data; while the worst one among them, i.e. LigScore, basically produced no appreciable correlation ($R = 0.344$). This observation confirms our statement that a preparing validation of available docking/scoring methods on the given target is critical for the success of subsequent analyses. It is not the aim of this study to explore in details why the performance of X-Score was the best among all. It seems that X-Score has a more balanced treatment of hydrogen bonds and hydrophobic contacts between protein and ligand. Note that the performance of GoldScore was also acceptable in this test ($R = 0.690$), which is an additional support for conducting molecular docking in our study with GOLD/GoldScore.

3.2. Molecular design and preliminary evaluation

The primary goal of our study is to design some reasonable molecules able to bind to the main binding site as well as the adjacent 150-cavity as potential N1 inhibitors. Our hypothesis is that such compounds may achieve better selectivity towards N1 other than other subtypes of neuraminidases and thus have potential advantages in clinical applications. As mentioned in Section 1, Garcia-Sosa et al. [19] and McCammon et al. [20] published their studies recently, which all aimed at discovering multiple-site binding N1 inhibitors. Nevertheless, both studies proposed some chemical structures for this aim through virtual screening. None of those chemical structures, unfortunately, has been validated in biological assays against any type of neurami-



Scheme 2. Twelve molecules selected from FDA-approved drugs with suitable fragments fitting to the 150-cavity on the open conformation of N1 (the binding fragments are indicated in red).

Table 3

Computed binding affinities of our designed molecules targeting at the open conformation of N1.

Name	Chemical structure	Binding scores				Binding free energies by MM-PB/SA (kcal/mol)
		Based on docked binding poses		Based on the last MD snapshots		
		GoldScore	X-Score	GoldScore	X-Score	
Tamiflu		65.85 ^a 75.59 ^b	5.39 ^a 5.86 ^b	73.86 ^a 77.64 ^b	5.83 ^a 5.87 ^b	−12.79 ^a −25.97 ^b
CP01		77.13	7.08	69.67	6.83	−12.15
CP02 ^c		81.67	6.64	47.38	5.45	2.97
CP03 ^c		86.04	6.35	N/A	N/A	N/A
CP04 ^c		54.96	5.82	N/A	N/A	N/A
CP04_1		78.81	6.19	53.50	6.32	−7.03
CP05 ^c		83.31	6.70	52.43	6.35	4.98
CP05_1		84.43	6.81	74.37	6.59	−9.43
CP05_2		83.92	6.79	65.28	6.58	−16.56

Table 3 (Continued)

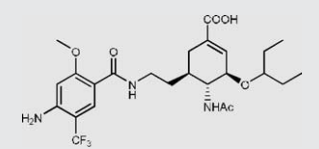
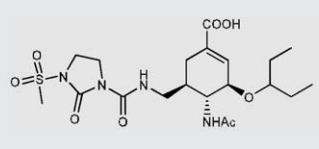
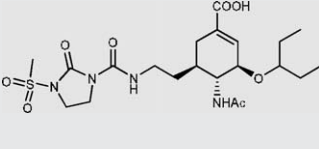
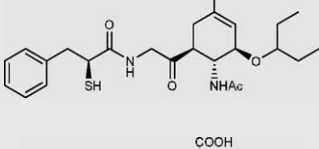
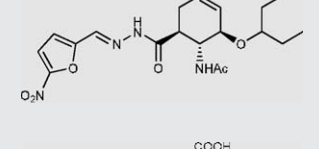
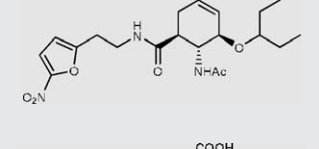
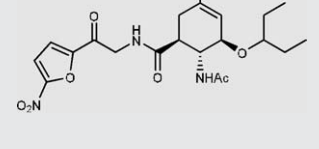
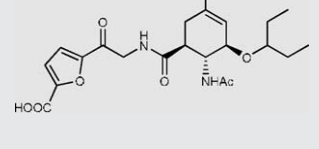
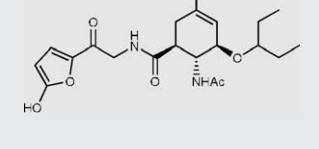
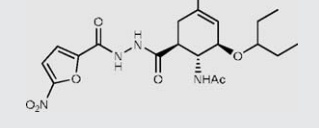
Name	Chemical structure	Binding scores				Binding free energies by MM-PB/SA (kcal/mol)
		Based on docked binding poses		Based on the last MD snapshots		
		GoldScore	X-Score	GoldScore	X-Score	
CP05_3		81.98	6.75	51.17	6.65	−6.49
CP06 ^c		65.82	6.35	N/A	N/A	N/A
CP06_1		82.04	6.23	83.03	6.56	−23.83
CP07		90.90	6.72	86.15	6.62	−18.16
CP08		95.59	6.75	82.76	6.77	−23.14
CP08_1		91.87	6.44	89.23	6.90	−26.95
CP08_2		90.69	6.69	80.27	6.62	−28.76
CP08_3		95.23	6.73	95.14	6.83	−16.89
CP08_4		82.88	6.38	104.61	7.24	−31.05
CP08_5		87.22	6.93	58.45	6.45	−19.97

Table 3 (Continued)

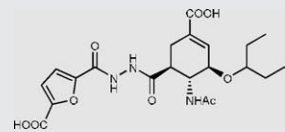
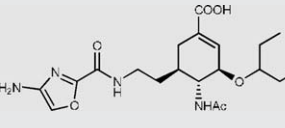
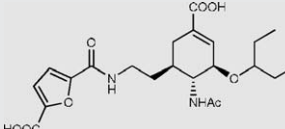
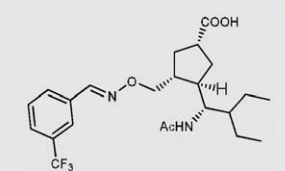
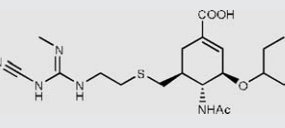
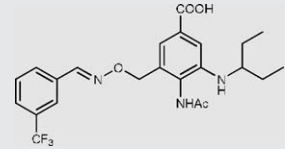
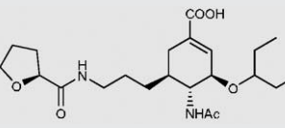
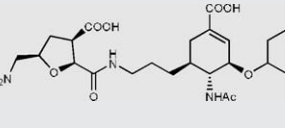
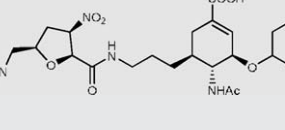
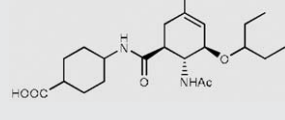
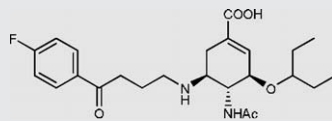
Name	Chemical structure	Binding scores				Binding free energies by MM-PB/SA (kcal/mol)
		Based on docked binding poses		Based on the last MD snapshots		
		GoldScore	X-Score	GoldScore	X-Score	
CP08_6		97.60	6.88	59.70	6.50	−12.31
CP08_7		86.64	6.16	71.46	5.84	−11.96
CP08_8		80.37	6.57	67.87	5.95	−16.47
CP09 ^c		82.22	6.96	N/A	N/A	N/A
CP10		85.46	6.15	70.40	5.73	−8.40
CP11		83.20	6.93	65.90	7.01	−4.88
CP12 ^c		80.39	6.10	60.91	5.71	2.67
CP12_1		90.81	6.21	67.89	6.01	−12.06
CP12_2		91.77	6.47	90.14	6.56	−28.42
CP13 ^c		63.05	6.31	N/A	N/A	N/A

Table 3 (Continued)

Name	Chemical structure	Binding scores				Binding free energies by MM-PB/SA (kcal/mol)
		Based on docked binding poses		Based on the last MD snapshots		
		GoldScore	X-Score	GoldScore	X-Score	
CP14		80.23	6.55	57.73	5.46	−6.03
CP15		85.86	6.87	63.96	6.12	−13.78

^a Computed on the open conformation of N1.^b Computed on the closed conformation of N1.^c These molecules either did not form stable complexes with N1 or are predicted to have unfavorable (positive) binding free energies by MM-PB/SA.

nidases before. Thus, their designs are still risky. In contrast, we chose to develop the structure of Tamiflu to achieve the same goal. Tamiflu is a logical choice. As indicated by the crystal structures of N1–Tamiflu complexes, Tamiflu is able to bind to the main binding site in both the closed and the open conformations. Obviously, the primary feature of any effective N1 inhibitor is a good binding to the main binding site rather than the 150-cavity or the 430-cavity. Utilizing Tamiflu as the core structure of newly designed molecules will hopefully retain the critical interactions with N1 at least at the main binding site. The new molecules designed so may also have potential advantages in terms of safety issues since Tamiflu has been widely used for the treatment of both Influenza virus A and B.

The first step of our design was to dock the 1046 FDA-approved drug molecules onto the open conformation of N1 using GOLD/GoldScore. A total of 12 molecules were selected from the screening results according to the criteria given in Section 2 (Scheme 2). Interestingly, none of our selections overlapped with Garcia-Sosa's selections from the same database targeting at the same target structure, indicating that the final outcomes of a virtual screening effort are actually affected by many factors. The 12 molecules selected by us all have certain chemical fragments occupying the 150-cavity as predicted by our molecular docking. Notably, most of these fragments contain multiple hetero-atoms. This common feature makes them form possible hydrogen bonds with the polar residues around the 150-cavity, including Arg118, Thr135, Asn136, Asp151, Arg156, and Thr439. Moreover, these selected molecules typically have an amide or other type of reasonable chemical groups linking the fragment occupying the 150-cavity and the rest parts of these molecules, and thus the subsequent truncations on chemical structures can be made accordingly at such positions. The second step of our design was to truncate the fragments occupying the 150-cavity and to connect them to the core structure of Tamiflu by making appropriate chemical bonds. A total of 15 molecules were manually designed in this way, and another 15 molecules were designed by making some intuitive modifications on them, aiming at improving their binding affinities to N1 (Table 3).

Note that in structure-based drug design, modification of a given lead structure can be conducted automatically with the aid of a *de novo* design program by assembling some chemical fragments onto it. Nevertheless, the outcomes produced by this approach may not be “drug-like” or simply unfeasible for organic synthesis. As indicated conceptually in Fig. 3, our approach is also about assembling some chemical fragments onto a given core structure. The difference is that the chemical fragments used in our design

are truncated directly from some known compounds. Therefore, the synthetical feasibility of our designed molecules is in principle better than *de novo* structures. In addition, choosing the FDA-approved drugs as the source for truncating such fragments improves the “drug-likeness” of our designed molecules. These fragments hopefully will not cause toxic side effects by themselves or their metabolites.

The binding poses of these designed molecules were then obtained through molecular docking with GOLD/GoldScore using the same parameter setting given in Section 2. Based on these predicted binding poses, the binding affinities of these designed molecules were evaluated by using the X-Score and GoldScore scoring function. The aim of this evaluation was to quickly filter some designed molecules which were unlikely to form stable complexes with N1 on the basis of some rough criteria. For this purpose, two criteria were proposed: (i) The brought-in fragment should not largely affect the original binding mode of the core structure. That means that the main hydrogen bonds formed between the carboxyl group on the core structure and three arginine amino acid residues nearby (Arg118, Arg292 and Arg371)

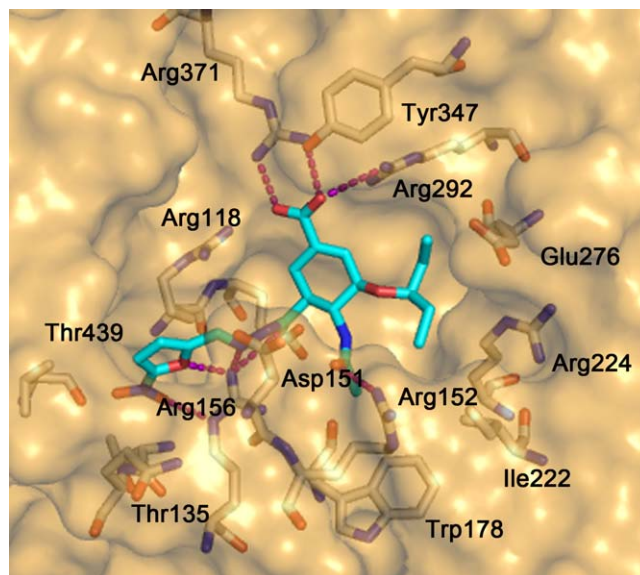


Fig. 6. Predicted binding mode of the designed molecule CP08. The purple dashes denote the formed hydrogen bonding interactions between N1 and CP08.

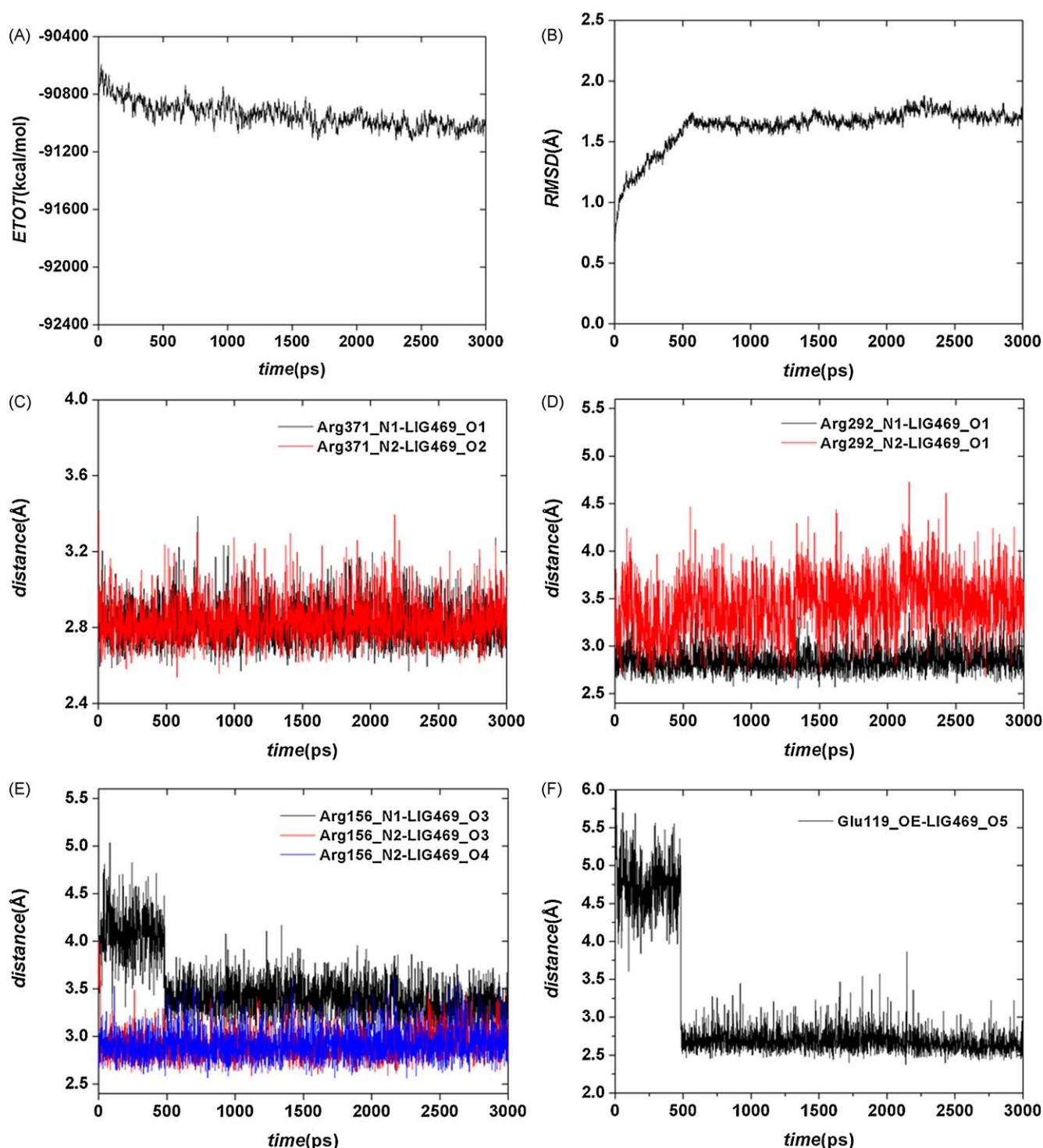
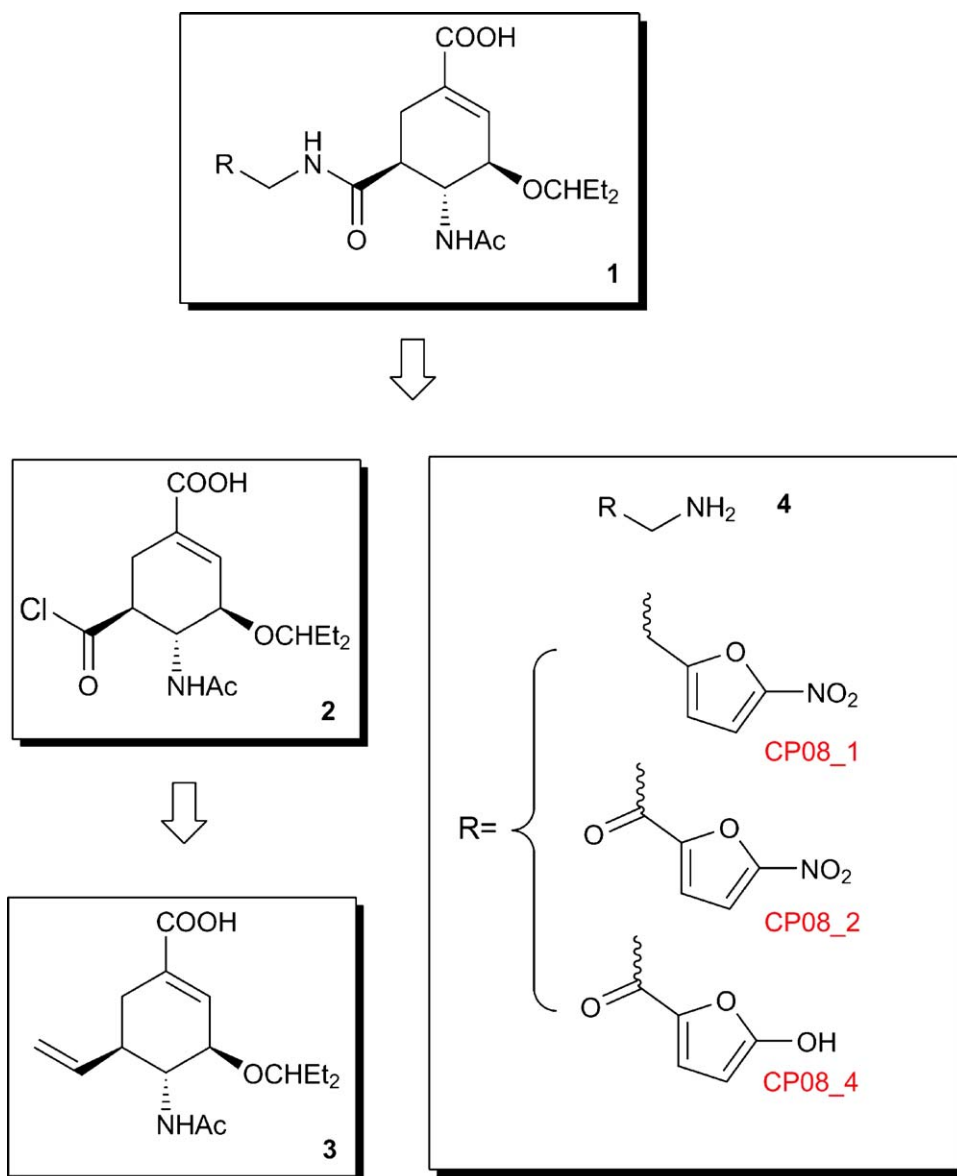


Fig. 7. MD simulation results of the N1-CP08_4 complex. (A) Total energy of the system. (B) RMSD of all heavy atoms in the complex. (C) Hydrogen bonds between Arg371 and the carboxylic group (atoms O1, O2) on CP08_4. (D) Hydrogen bond between Arg292 and atom O1 on CP08_4. (E) Hydrogen bonds between Arg156 and atoms O3 and O4 on CP08_4. (F) Hydrogen bond between Glu119 and atom O5 on CP08_4. Atom annotations on CP08_4 are given in Fig. 8.

still retain. (ii) Their binding scores should not be lower than the counterparts of the N1-Tamiflu complex in the open conformation (GoldScore = 66; X-Score = 5.50).

According to the above criteria, most of the newly designed molecules could form desired interactions with the open conformation of N1. As shown in Table 3, most of these molecules have promising binding affinities predicted by both GoldScore and X-Score. Only three molecules, including CP04, CP06 and CP13,

were discarded due to weak binding to N1. In particular, molecule CP08 drew our attention. The core structure in this molecule keeps the desired hydrogen bonds with the arginine residues on N1 as Tamiflu (see Fig. 6). In addition, the oxygen atoms in the nitro group and the furan ring, together with the carbonyl group on the linker, formed new hydrogen bonding networks with Arg156 near the 150-cavity. This may promote the binding of CP08 to N1. In fact, both GoldScore and X-Score predicted better binding affinities of

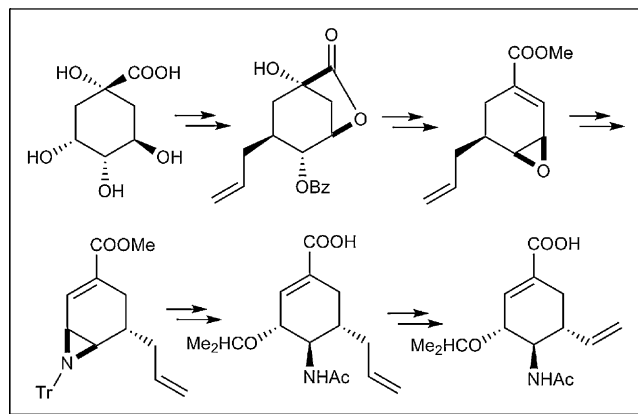


Scheme 3. Retrosynthetic analysis of CP08 and its derivatives.

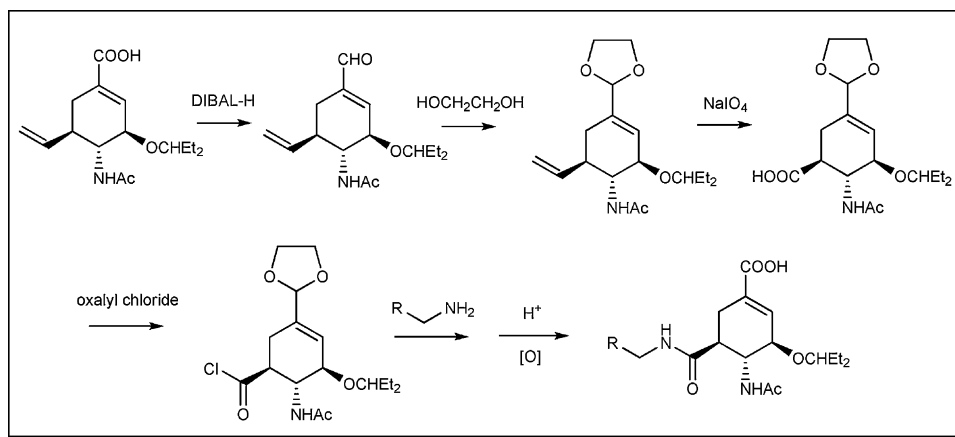
this molecule than that of Tamiflu (GoldScore = 95.59; X-Score = 6.75). This molecule stands a good chance to be a potential inhibitor for N1.

3.3. Further evaluation through MD simulations and binding free energy computations

The three-dimensional structure of N1 was fixed in our molecular docking studies described above. This simplification may be faulty since, as indicated by the experimentally observed open and closed conformations of N1, the structure of N1 is intrinsically flexible to certain extents. In order to account for the flexibility of the N1 structure, MD simulations were conducted to refine the complex structures formed between N1 and all our designed molecules. The conformational ensembles produced by MD simulations were also used as inputs for the subsequent MM-PB/SA computation, which was employed as an alternative approach for predicting the binding affinities of designed molecules.



Scheme 4. A previously reported synthesis method of an analogue of compound 3 (Ref. [59]).



Scheme 5. A proposed synthetic route for CP08 and its derivatives.

Our results show that most of these small molecules formed stable complexes with N1 after 3 ns MD simulation. This can be demonstrated by monitoring the fluctuations of total energies, RMSD values, and major hydrogen bonding interactions in those complexes along the MD trajectories (see the [Supporting Information](#)). The binding free energy of Tamiflu to the open conformation of N1 predicted by our MM-PB/SA computation was -12.79 kcal/mol ([Table 3](#)). About half of our designed molecules gave comparable or better binding affinities to the open conformation of N1 than Tamiflu ([Table 3](#)). In particular, three molecules derived from CP08, i.e. CP08_1, CP08_2, and CP08_4, formed tight complexes with the open conformation of N1. Their predicted binding free energies ($\Delta G_{\text{cal,CP08}_1} = -26.95$ kcal/mol, $\Delta G_{\text{cal,CP08}_2} = -28.76$ kcal/mol, and $\Delta G_{\text{cal,CP08}_4} = -31.05$ kcal/mol) were even lower than that of the N1–Tamiflu complex in its closed conformation ($\Delta G_{\text{cal,Tamiflu}} = -25.97$ kcal/mol). The high predicted binding affinities of these several molecules can be well understood. Let us take CP08_4 as an example. The RMSD fluctuation curve shown in [Fig. 7A](#) and [B](#) indicates that the N1–CP08_4 complex went stable after 0.6 ns and remained in a steady state during the rest 2.4 ns simulation. The critical hydrogen bonds between the core structure in CP08_4 and N1 were well retained during the entire MD simulation ([Fig. 7C](#) and [D](#)). Besides, the oxygen atom in the furan ring, together with the hydroxyl group,

formed new hydrogen bonding networks with Arg156 and Glu119 near the 150-cavity ([Fig. 7E](#) and [F](#)). These additional interactions largely improved the binding affinity of this complex. The final binding mode of CP08_4 after MD simulation is illustrated in [Fig. 8](#).

In contrast, two molecules (CP03 and CP09) could not form stable interactions with N1 during 3 ns MD simulations; while three other molecules (CP02, CP05, and CP12) gave positive binding free energies by MM-PB/SA method, though in our preliminary evaluation they were predicted to have good binding affinities by scoring functions ([Table 3](#)). This observation confirms that applying another approach to binding affinity prediction is necessary for obtaining reliable results. After eliminating these unpromising designs, 22 designed molecules could form stable interactions with the open conformation of N1, occupying both the main binding site and the 150-cavity. Some of them are predicted to have better binding affinities than that of Tamiflu, which fulfills our original goal of this study.

3.4. Proposed synthetic routes for selected compounds

As discussed above, CP08 and its direct derivatives (CP08_1, CP08_2 and CP08_4) in particular were predicted to form tight complexes with N1 in its open conformation, which may be eventually developed into a new class of N1 inhibitors. Herein, we also discuss the feasible synthetic route of these designed molecules as another evaluation of their usefulness.

One can see that all these compounds are composed of the Tamiflu scaffold, an amide linker, and a substituted furan moiety. The retrosynthetic analysis of these compounds is proposed in [Scheme 3](#). The target compound **1** can be obtained from compounds **2** and **4** through a condensation reaction. Obviously, preparation of compound **3**, i.e. the precursor of compound **2**, is the key step in the synthesis of the target compounds. As a matter of fact, synthesis of an analogue of it has been previously reported in the literature [59]. The brief synthetic route is shown in [Scheme 4](#). Compound **4** can be derived from furan. Synthesis of some analogues has also been reported [60–62]. The feasible synthetic method for linking the Tamiflu scaffold and the furan moiety is given in [Scheme 5](#) [63]. Considering the acid intermediate in the condensation reaction, compound **3** should be reduced to aldehyde first by diisobutylaluminum hydride (DIBAL-H), and then protected with glycol. After that, the C=C double bond outside the ring is oxidized and transformed to acid chloride. The intermediate compound then reacts with compound **4** through condensation. Finally, eliminating the protecting group and oxidizing aldehyde to carboxyl group gives the target compounds.

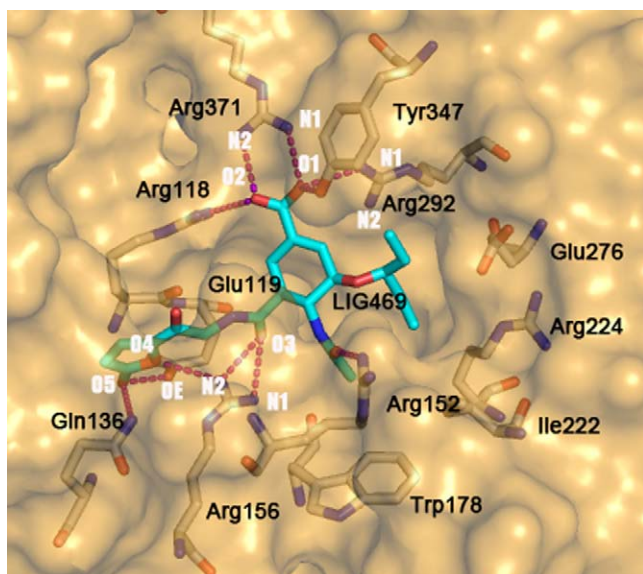


Fig. 8. Binding mode of CP08_4 observed in the last snapshot of MD simulation.

4. Conclusions

We have designed some derivatives of Tamiflu targeting at the open conformation of N1 through a combination of molecular docking, molecular dynamics simulation and binding affinity computation. The core structure of Tamiflu was utilized to occupy the main binding site on N1. Some chemical fragments, which could fit into the 150-cavity, were selected from a virtual screening trial of over 1000 FDA-approved drugs. These fragments were then installed onto the core structure of Tamiflu via proper chemical bonds to produce a total of 30 new molecules. Our study actually represents an alternative approach to the structure-based optimization of a given lead compound. Molecules designed through this approach have certain advantages in terms of synthetic feasibility and drug-likeness. Many of our designed molecules were predicted to form stable complexes with N1, exhibiting binding affinities comparable or even better than that of Tamiflu. In particular, a class of molecules with a substituted furan moiety occupying the 150-cavity, i.e. CP08 and its derivatives, seem to be very promising. These molecules may be eventually developed into new N1 inhibitors with better biological activities and specificities against avian influenza virus H5N1. We herein reveal our results so that other researchers who have the necessary chemical and biological resources may test these ideas.

Acknowledgments

The authors are grateful to the financial supports from the Chinese National Natural Science Foundation (Grants No. 20772149 & No. 90813006), the Chinese Ministry of Science and Technology (the 863 high-tech project, Grant No. 2006AA02Z337), and the Science and Technology Commission of Shanghai Municipality (Grant No. 074319113). The authors are also grateful to Prof. Zhujun Yao at the Shanghai Institute of Organic Chemistry for his helpful discussion.

Appendix A. Supplementary data

Supplementary data associated with this article can be found, in the online version, at [doi:10.1016/j.jmgm.2009.07.001](https://doi.org/10.1016/j.jmgm.2009.07.001).

References

- [1] J.N.S.S. Couceiro, J.C. Paulson, L.G. Baum, Influenza virus strains selectively recognize sialyloligosaccharides on human respiratory epithelium, the role of the host cell in selection of hemagglutinin receptor specificity, *Virus Res.* 29 (1993) 155–165.
- [2] C. Liu, M.C. Eichelberger, R.W. Compans, G.M. Air, Influenza type A virus neuraminidase does not play a role in viral entry, replication, assembly, or budding, *J. Virol.* 69 (1995) 1099–1106.
- [3] World Health Organization, A revision of the system of nomenclature for influenza viruses: a WHO memorandum, *Bull. World Health Organ.* 58 (1980) 585–591.
- [4] C. Bender, H. Hall, J. Huang, A. Klimov, N. Cox, A. Hay, V. Gregory, K. Cameron, W. Lim, K. Subbarao, Characterization of the surface proteins of influenza A (H5N1) viruses isolated from humans in 1997–1998, *Virology* 254 (1999) 115–123.
- [5] W. Weis, J.H. Brown, S. Cusack, J.C. Paulson, J.J. Skehel, D.C. Wiley, Structure of the influenza virus haemagglutinin complexed with its receptor, sialic acid, *Nature* 333 (1988) 426–431.
- [6] M. von Itzstein, W.-Y. Wu, G.B. Kok, M.S. Pegg, J.C. Dyason, B. Jin, T.V. Phan, M.L. Smythe, H.F. White, S.W. Oliver, P.M. Colman, J.N. Varghese, D.M. Ryan, J.M. Woods, R.C. Bethell, V.J. Hotham, J.M. Cameron, C.R. Penn, Rational design of potent sialidase-based inhibitors of influenza virus replication, *Nature* 363 (1993) 418–423.
- [7] C.U. Kim, W. Lew, M.A. Williams, H. Liu, L. Zhang, S. Swaminathan, N. Bischofberger, M.S. Chen, D.B. Mendel, C.Y. Tai, W.G. Laver, R.C. Stevens, Influenza neuraminidase inhibitors possessing a novel hydrophobic interaction in the enzyme active site: design, synthesis, and structural analysis of carbocyclic sialic acid analogues with potent anti-influenza activity, *J. Am. Chem. Soc.* 119 (1997) 681–690.
- [8] P.A. Reece, Neuraminidase inhibitor resistance in influenza viruses, *J. Med. Virol.* 79 (2007) 1577–1586.
- [9] Y.S. Babu, P. Chand, S. Bantia, P. Kotian, A. Dehghani, Y. El-Kattan, T.-H. Lin, T.L. Hutchison, A.J. Elliott, C.D. Parker, S.L. Ananth, L.L. Horn, G.W. Laver, J.A. Montgomery, BCX-1812(RWJ-270201): discovery of a novel, highly potent, orally active, and selective influenza neuraminidase inhibitor through structure-based drug design, *J. Med. Chem.* 43 (2000) 3482–3486.
- [10] N.R. Taylor, A. Cleasby, O. Singh, T. Skarzynski, A.J. Wonacott, P.W. Smith, S.L. Solliis, P.D. Howes, P.C. Cherry, R. Bethell, P. Colman, J. Varghese, Dihydropyrancarboxamides related to zanamivir: a new series of inhibitors of influenza virus sialidases. 2. Crystallographic and molecular modeling study of complexes of 4-amino-4H-pyran-6-carboxamides and sialidase from influenza virus types A and B, *J. Med. Chem.* 41 (1998) 798–807.
- [11] C.J. Maring, V.S. Stoll, C. Zhao, M. Sun, A.C. Krueger, K.D. Stewart, D.L. Madigan, W.M. Kati, Y. Xu, R.J. Carrick, D.A. Montgomery, A. Kempf-Grote, K.C. Marsh, A. Molla, K.R. Steffy, H.L. Sham, W.G. Laver, Y.-G. Gu, D.J. Kempf, W.E. Kohlbrener, Structure-based characterization and optimization of novel hydrophobic binding interactions in a series of pyrrolidine influenza neuraminidase inhibitors, *J. Med. Chem.* 48 (2005) 3980–3990.
- [12] J.C. Wilson, M. von Itzstein, Recent strategies in the search for new anti-influenza therapies, *Curr. Drug Targets* 4 (2003) 389–408.
- [13] C.U. Kim, W. Lew, M.A. Williams, H. Wu, L. Zhang, X. Chen, P.A. Escarpe, D.B. Mendel, W.G. Laver, R.C. Stevens, Structure-activity relationship studies of novel carbocyclic influenza neuraminidase inhibitors, *J. Med. Chem.* 41 (1998) 2451–2460.
- [14] G.T. Wang, Y. Chen, S. Wang, R. Gentles, T. Sowin, W. Kati, S. Muchmore, V. Giranda, K. Stewart, H. Sham, D. Kempf, W.G. Laver, Design, synthesis and structural analysis of influenza neuraminidase inhibitors containing pyrrolidine cores, *J. Med. Chem.* 44 (2001) 1192–1201.
- [15] W.J. Brouillette, S.N. Bajpai, S.M. Ali, S.E. Velu, V.R. Atigadda, B.S. Lommer, J.B. Finley, M. Luo, G.M. Air, Pyrrolidinobenzoic acid inhibitors of influenza virus neuraminidase: modifications of essential pyrrolidinone ring substituents, *Bioorg. Med. Chem.* 11 (2003) 2739–2749.
- [16] P. Chand, Y.S. Babu, S. Bantia, S. Rowland, A. Dehghani, P.L. Kotian, T.L. Hutchison, S. Ali, W. Brouillette, Y. El-Kattan, T.-H. Lin, Syntheses and neuraminidase inhibitory activity of multisubstituted cyclopentane amide derivatives, *J. Med. Chem.* 47 (2004) 1919–1929.
- [17] P. Chand, P.L. Kotian, P.E. Morris, S. Bantia, D.A. Walsh, Y.S. Babu, Synthesis and inhibitory activity of benzoic acid and pyridine derivatives on influenza neuraminidase, *Bioorg. Med. Chem.* 13 (2005) 2665–2678.
- [18] R.J. Russell, L.F. Haire, D.J. Stevens, P.J. Collins, Y.P. Lin, G.M. Blackburn, A.J. Hey, S.J. Gamblin, J.J. Skehel, The structure of H5N1 avian influenza neuraminidase suggests new opportunities for drug design, *Nature* 443 (2006) 45–49.
- [19] A.T. Garcia-Sosa, S. Sild, U. Maran, Design of multi-binding-site inhibitors, ligand efficiency and consensus screening of avian influenza H5N1 wild-type neuraminidase and of the oseltamivir-resistant H274Y variant, *J. Chem. Inf. Model.* 48 (2008) 2074–2080.
- [20] L.S. Cheng, R.E. Amaro, D. Xu, W.W. Li, P.W. Arzberger, J.A. McCammon, Ensemble-based virtual screening reveals potential antiviral compounds for avian influenza neuraminidase, *J. Med. Chem.* 51 (2008) 3878–3894.
- [21] C. Bissantz, G. Folkers, D. Rognan, Protein-based virtual screening of chemical databases. 1. Evaluation of different docking/scoring combinations, *J. Med. Chem.* 43 (2000) 4759–4767.
- [22] R. Wang, Y. Lu, S. Wang, Comparative evaluation of 11 scoring functions for molecular dockings, *J. Med. Chem.* 46 (2003) 2287–2303.
- [23] R. Wang, Y. Lu, X. Fang, S. Wang, An extensive test of 14 scoring functions using the PDBbind refined set of 800 protein–ligand complexes, *J. Chem. Inf. Comput. Sci.* 44 (2004) 2114–2125.
- [24] G.L. Warren, C.W. Andrews, A.-M. Capelli, B. Clarke, J. LaLonde, M.H. Lambert, M. Lindvall, N. Nevins, S.F. Semus, S. Senger, G. Tedesco, I.D. Wall, J.M. Woolven, C.E. Peishoff, M.S. Head, A critical assessment of docking programs and scoring functions, *J. Med. Chem.* 49 (2006) 5912–5931.
- [25] W. Lew, H. Wu, D.B. Mendel, P.A. Escarpe, X. Chen, W.G. Laver, B.J. Graves, C.U. Kim, A new series of C3-aza carbocyclic influenza neuraminidase inhibitors: synthesis and inhibitory activity, *Bioorg. Med. Chem. Lett.* 8 (1998) 3321–3324.
- [26] H.M. Berman, J. Westbrook, Z. Feng, G. Gilliland, T.N. Bhat, H. Weissig, I.N. Shindyalov, P.E. Bourne, The Protein Data Bank, *Nucleic Acids Res.* 28 (2000) 235–242.
- [27] G. Jones, P. Willett, R.C. Glen, Molecular recognition of receptor sites using a genetic algorithm with a description of desolvation, *J. Mol. Biol.* 245 (1995) 43–53.
- [28] M.L. Verdonk, J.C. Cole, M.J. Hartshorn, C.W. Murray, R.D. Taylor, Improved protein–ligand docking using GOLD, *Proteins* 52 (2003) 609–623.
- [29] M.D. Eldridge, C.W. Murray, T.R. Auton, G.V. Paolini, R.P. Mee, Empirical scoring functions. I. The development of a fast empirical scoring function to estimate the binding affinity of ligands in receptor complexes, *J. Comput. Aided Mol. Des.* 11 (1997) 425–445.
- [30] C.M. Venkatachalam, X. Jiang, T. Oldfield, M. Waldman, LigandFit: a novel method for the shape-directed rapid docking of ligands to protein active sites, *J. Mol. Graph. Model.* 21 (2003) 289–307.
- [31] D.K. Gehlhaar, G.M. Verkhivker, P.A. Rejto, C.J. Sherman, D.B. Fogel, L.J. Fogel, S.T. Freer, Molecular recognition of the inhibitor AG-1343 by HIV-1 protease: conformationally flexible docking by evolutionary programming, *Chem. Biol.* 2 (1995) 317–324.
- [32] I. Muegge, Y.C. Martin, A general and fast scoring function for protein–ligand interactions: a simplified potential approach, *J. Med. Chem.* 42 (1999) 791–804.

- [33] A. Krammer, P.D. Kirchhoff, X. Jiang, C.M. Venkatachalam, M. Waldman, LigScore: a novel scoring function for predicting binding affinities, *J. Mol. Graph. Model.* 23 (2005) 395–407.
- [34] H.-J. Bohm, The development of a simple empirical scoring function to estimate the binding constant for a protein–ligand complex of known three-dimensional structure, *J. Comput. Aided Mol. Des.* 8 (1994) 243–256.
- [35] A.N. Jain, Scoring noncovalent protein–ligand interactions: a continuous differentiable function to compute binding affinities, *J. Comput. Aided Mol. Des.* 10 (1996) 427–440.
- [36] R. Wang, L. Lai, S. Wang, Further development and validation of empirical scoring functions for structure-based affinity prediction, *J. Comput. Aided Mol. Des.* 16 (2002) 11–26.
- [37] R.D. Cramer III, D.E. Patterson, J.D. Bunce, Comparative molecular field analysis (CoMFA). 1. Effect of shape on binding of steroids to carrier proteins, *J. Am. Chem. Soc.* 110 (1988) 5959–5967.
- [38] M. Verdondk, M.J. Hartshorn, Structure-guided fragment screening for lead discovery, *Curr. Opin. Drug Discov. Dev.* 7 (2004) 404–410.
- [39] P.J. Hajduk, J. Greer, A decade of fragment-based drug design: strategic advances and lessons learned, *Nat. Rev. Drug Discov.* 6 (2007) 211–219.
- [40] A. Ciulli, C. Abell, Fragment-based approaches to enzyme inhibition, *Curr. Opin. Biotechnol.* 18 (2007) 489–496.
- [41] M. Congreve, G. Chessari, D. Tisi, A.J. Woodhead, Recent developments in fragment-based drug discovery, *J. Med. Chem.* 51 (2008) 3661–3680.
- [42] D.S. Wishart, C. Knox, A.C. Guo, S. Shrivastava, M. Hassanali, P. Stothard, Z. Chang, J. Woolsey, DrugBank: a comprehensive resource for in silico drug discovery and exploration, *Nucleic Acids Res.* 34 (2006) D668–D672.
- [43] M.J. Frisch, G.W. Trucks, H.B. Schlegel, G.E. Scuseria, M.A. Robb, J.R. Cheeseman, J.A. Montgomery Jr., T. Vreven, K.N. Kudin, J.C. Burant, J.M. Millam, S.S. Iyengar, J. Tomasi, V. Barone, B. Mennucci, M. Cossi, G. Scalmani, N. Rega, G.A. Petersson, H. Nakatsuji, M. Hada, M. Ehara, K. Toyota, R. Fukuda, J. Hasegawa, M. Ishida, T. Nakajima, Y. Honda, O. Kitao, H. Nakai, M. Klene, X. Li, J.E. Knox, H.P. Hratchian, J.B. Cross, V. Bakken, C. Adamo, J. Jaramillo, R. Gomperts, R.E. Stratmann, O. Yazyev, A.J. Austin, R. Cammi, C. Pomelli, J.W. Ochterski, P.Y. Ayala, K. Morokuma, G.A. Voth, P. Salvador, J.J. Dannenberg, V.G. Zakrzewski, S. Dapprich, A.D. Daniels, M.C. Strain, O. Farkas, D.K. Malick, A.D. Rabuck, K. Raghavachari, J.B. Foresman, J.V. Ortiz, Q. Cui, A.G. Baboul, S. Clifford, J. Cioslowski, B.B. Stefanov, G. Liu, A. Liashenko, P. Piskorz, I. Komaromi, R.L. Martin, D.J. Fox, T. Keith, M.A. Al-Laham, C.Y. Peng, A. Nanayakkara, M. Challacombe, P.M.W. Gill, B. Johnson, W. Chen, M.W. Wong, C. Gonzalez, J.A. Pople, Gaussian 03, Revision C.02, Gaussian, Inc., Wallingford, CT, 2004.
- [44] C.I. Bayly, P. Cieplak, W.D. Cornell, P.A. Kollman, A well-behaved electrostatic potential based method using charge restraints for deriving atomic charges: the RESP model, *J. Phys. Chem.* 97 (1993) 10269–10280.
- [45] D.A. Case, T.A. Darden, T.E. Cheatham, C.L. Simmerling, J. Wang, R.E. Duke, R. Luo, K.M. Merz, D.A. Pearlman, M. Crowley, R.C. Walker, W. Zhang, B. Wang, S. Hayik, A. Roitberg, G. Seabra, K.F. Wong, F. Paesani, X. Wu, S. Brozell, V. Tsui, H. Gohlke, L. Yang, C. Tan, J. Mongan, V. Hornak, G. Cui, P. Beroza, D.H. Mathews, C. Schafmeister, W.S. Ross, P.A. Kollman, AMBER 9, University of California, San Francisco, 2006.
- [46] H.J.C. Berendsen, J.P.M. Postma, W.F. van Gunsteren, A. DiNola, J.R. Haak, Molecular dynamics with coupling to an external bath, *J. Chem. Phys.* 81 (1984) 3684–3690.
- [47] T. Darden, D. York, L. Pedersen, Particle mesh Ewald—an $N \log(N)$ method for Ewald sums in large systems, *J. Chem. Phys.* 98 (1993) 10089–10092.
- [48] S. Miyamoto, P.A. Kollman, SETTLE: an analytical version of the SHAKE and RATTLE algorithm for rigid water models, *J. Comput. Chem.* 13 (1992) 952–962.
- [49] P.A. Kollman, I. Massova, C. Reyes, B. Kuhn, S. Huo, L. Chong, M. Lee, T. Lee, Y. Duan, W. Wang, O. Donini, P. Cieplak, J. Srinivasan, D.A. Case, T.E. Cheatham, Calculating structures and free energies of complex molecules: combining molecular mechanics and continuum models, *Acc. Chem. Res.* 33 (2000) 889–897.
- [50] W. Wang, W.A. Lim, A. Jakalian, J. Wang, J.M. Wang, R. Luo, C.T. Bayly, P.A. Kollman, An analysis of the interactions between the Sem-5 SH3 domain and its ligands using molecular dynamics, free energy calculations, and sequence analysis, *J. Am. Chem. Soc.* 123 (2001) 3986–3994.
- [51] J.M. Wang, P. Morin, W. Wang, P.A. Kollman, Use of MM-PBSA in reproducing the binding free energies to HIV-1 RT of TIBO derivatives and predicting the binding mode to HIV-1 RT of efavirenz by docking and MM-PBSA, *J. Am. Chem. Soc.* 123 (2001) 5221–5230.
- [52] W. Wang, P.A. Kollman, Computational study of protein specificity: the molecular basis of HIV-1 protease drug resistance, *Proc. Natl. Acad. Sci. U.S.A.* 98 (2001) 14937–14942.
- [53] T. Laitinen, J.A. Kankare, M. Perakyla, Free energy simulations and MM-PBSA analyses on the affinity and specificity of steroid binding to antiestradiol antibody, *Proteins* 55 (2004) 34–43.
- [54] F. Fogolari, E. Moroni, M. Wojciechowski, M. Baginski, L. Ragona, H. Molinari, MM/PBSA analysis of molecular dynamics simulations of bovine beta-lactoglobulin: free energy gradients in conformational transitions? *Proteins* 59 (2005) 91–103.
- [55] Y. Xu, R.X. Wang, A computational analysis of the binding affinities of FKBP12 inhibitors using the MM-PB/SA method, *Proteins* 64 (2006) 1058–1068.
- [56] H.J. Zou, C. Luo, S.X. Zheng, X.M. Luo, W.L. Zhu, K.X. Chen, J.H. Shen, H.L. Jiang, Molecular insight into the interaction between IFABP and PA by using MM-PBSA and alanine scanning methods, *J. Phys. Chem. B* 111 (2007) 9104–9113.
- [57] G. Lamm, Applications of Born–Oppenheimer direct dynamics, in: K.B. Lipkowitz, R. Larter, T.R. Cundari (Eds.), *Reviews in Computational Chemistry*, vol. 19, John Wiley & Sons Inc., New Jersey, 2003, pp. 147–365.
- [58] N.A. Baker, Biomolecular applications of Poisson–Boltzmann methods, in: K.B. Lipkowitz, R. Larter, T.R. Cundari (Eds.), *Reviews in Computational Chemistry*, vol. 21, John Wiley & Sons Inc., New Jersey, 2005, pp. 349–379.
- [59] S. Hanessian, J. Wang, D. Montgomery, V. Stoll, K.D. Stewart, W. Kati, C. Maring, D. Kempf, C. Hutchins, W.G. Laver, Design, synthesis and neuraminidase inhibitory activity of GS-4071 analogues that utilize a novel hydrophobic paradigm, *Bioorg. Med. Chem. Lett.* 12 (2002) 3425–3429.
- [60] M.M.Z. Owczarczyk, Direct formylation of nitroarenes via vicarious nucleophilic substitution of hydrogen, *Tetrahedron Lett.* 28 (1987) 3021–3022.
- [61] K. Hayes, C. O’Keefe, The nitration of 2-furyl methyl ketone: methyl 5-nitro-2-furyl ketone and 3,4-di-(2-furyl)-furoxan, *J. Org. Chem.* 19 (1954) 1897–1902.
- [62] A. Zwierzak, S. Pilichowska, Diethyl N-(t-butoxycarbonyl)-phosphoramidate: a new, useful substitute of phthalimide in Gabriel-type syntheses of primary amines, *Synthesis* 11 (1982) 922–924.
- [63] P.A. Stocks, P.G. Bray, V.E. Barton, M. Al-Helal, M. Jones, N.C. Araujo, P. Gibbons, S.A. Ward, R.H. Hughes, G.A. Biagini, J. Davies, R. Amewu, A.E. Mercer, G. Ellis, P.M. O’Neill, Evidence for a common non-heme chelatable-iron-dependent activation mechanism for semisynthetic and synthetic endoperoxide antimalarial drugs, *Angew. Chem. Int. Ed.* 46 (2007) 6278–6283.